Colloids and Surfaces A: Physicochem. Eng. Aspects 521 (2017) 133–140

Contents lists available at ScienceDirect

Colloids and Surfaces A: Physicochemical and Engineering Aspects

journal homepage: www.elsevier.com/locate/colsurfa

Formation of surfactant free microemulsions in the ternary system water/eugenol/ethanol

Alejandro Lucia[a], Pablo G. Argudo[b], Eduardo Guzmán[b], Ramón G. Rubio[b,c], Francisco Ortega[b,*]

[a] Centro de Investigaciones de Plagas e Insecticidas (UNIDEF/CITEDEF/CONICET), San Juan Bautista de La Salle 4397, B1603ALO-Villa Martelli-Buenos Aires, Argentina
[b] Departamento de Química Física I-Universidad Complutense de Madrid, Ciudad Universitaria s/n, 28040 Madrid, Spain
[c] Instituto Pluridisciplinar-Universidad Complutense de Madrid, Avd. Juan XXIII, 28040 Madrid, Spain

HIGHLIGHTS

- Water/eugenol/ethanol ternary mixtures present a complex phase diagram.
- System fulfilling the requirements for the appearance of the "pre-Ouzo" effect.
- Formation of miscible regions due to the co-solvency of ethanol.
- Ethanol can preferentially distribute between water and eugenol.
- Formation of a surfactantless microemulsion.

GRAPHICAL ABSTRACT

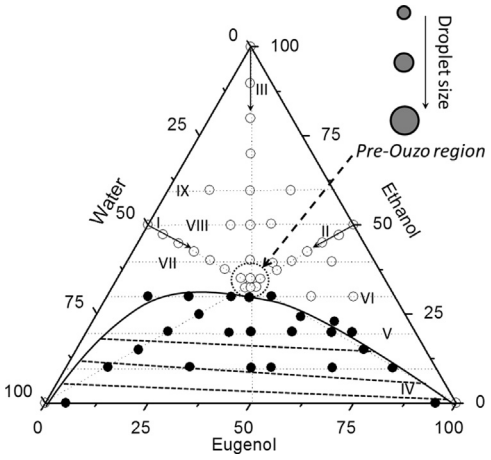

ARTICLE INFO

Article history:
Received 18 March 2016
Received in revised form 25 April 2016
Accepted 29 April 2016
Available online 13 May 2016

Keywords:
Surfactantless microemulsions
Dynamic Light Scattering
Ouzo effect

ABSTRACT

This works analyzes the aggregation phenomena occurring in a ternary mixture formed by two solvent mutually immiscible, water and eugenol, and a third solvent that can act as co-solvent with both, thus fulfilling the requirements for the appearance of the "pre-Ouzo" effect. The combination of visual observation of the samples and GC–MS allows us to draw a ternary phase diagram for the system. Dynamic Light Scattering (DLS) has provided information on the bulk aggregation occurring in the system, and also has given good insights in the destabilization of the pseudo-one phase region. The DLS measurements performed in different paths of the phase diagram have allowed us to establish a critical composition for destabilization of the one phase region, having equal content of the components. Stable microemulsions can be used for solubilization of a model insecticide, opening a new route for the fabrication of biosustainable formulations for insecticides.

1. Introduction

Microemulsions are ternary systems in which two liquid phases, generally water and an oil, and an amphiphilic molecule

* Corresponding author.
E-mail address: fortega@quim.ucm.es (F. Ortega).

http://dx.doi.org/10.1016/j.colsurfa.2016.04.062
0927-7757/

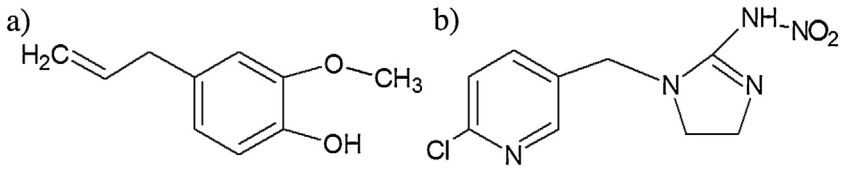

Scheme 1. Molecular formulas of eugenol (a) and imidacloprid (b).

(surfactant) lead to the spontaneous formation of a pseudo-single phase optically isotropic and thermodynamically stable liquid dispersion [1]. As well as other colloidal dispersions, microemulsion formation is strongly dependent on surfactant type and structure. In contrast to emulsions that are thermodynamically unstable systems, with drops with sizes larger than 0.1 μm, microemulsions contain very small droplets, with diameters typically within the 5–50 nm range, and are stable systems [2].

From the seminal studies by Smith et al. [3] to most recent studies [4–6] there is a strong controversy related to the possibility of obtaining surfactant free microemulsions. In recent years, several light and X-ray scattering studies and simulations have helped to shed light on the formation of this particular type of colloidal dispersion [7–9]. The formation of these surfactant free microemulsions occurs in ternary liquid mixtures containing two alcohols and is sometimes named as "pre-Ouzo" effect or spontaneous emulsification. The miscibility of two of the liquids (A and B), mutually immiscible, occurs in presence of a third liquid, C, which is simultaneously miscible with A and B, e.g. A: water. B: octanol and C: ethanol [8].

Klossek et al. [9] showed the formation of well-defined aggregates in the "pre-Ouzo" region for the system water/*n*-octanol/ethanol, more recently they found similar behaviour for the water/benzyl-alcohol/ethanol mixtures [6]. Diat et al. [7] found two distinct nanoscopic pseudo-phases, the first one being enriched in octanol, whereas the second one was water-rich. Using molecular dynamics simulations Schöttl et al. [8] demonstrated the formation of nano-structures (micelle-like aggregates) in the ternary mixture water/octanol/ethanol. The aggregates formed present different characteristics to those from simple critical density fluctuations. A similar behaviour was also found by Fisher et al. [4]. Despite the extensive research on this type of systems in recent years, so far it is not possible to predict whether three given liquids will lead to an "Ouzo" or "pre-Ouzo" region, and if so, in which concentration range [4,6–10].

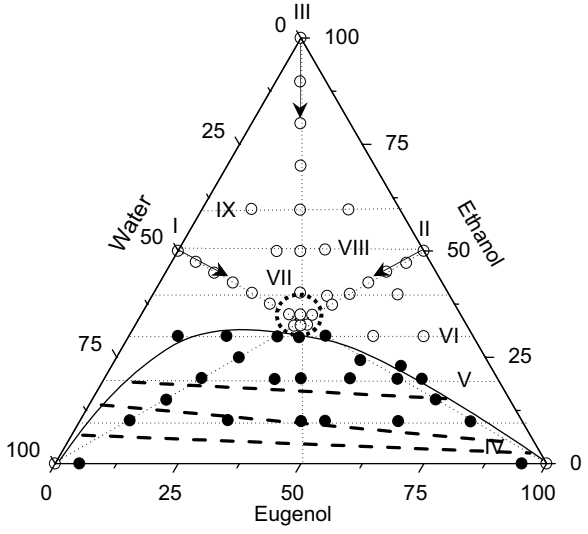

Fig. 1. Phase diagram for the system W/Eu/EtOH at 25 °C. The compositions of the different components are in weight fraction (wt%). The symbols indicate the different compositions studied: two phase compositions (●) and pseudo-single phase compositions (○). The solid curve line represents the limit of the separation between phase separated composition and pseudo-single phase composition, whereas the dotted circle defines the limit of the "pre-Ouzo" region. The dashes lines represent different tie lines obtained on the basis of GC–MS experiments. The different paths are identified with dotted lines and numbers from I to IX. The direction of the main paths studied are indicated with arrows (paths I–III).

The present study is focused on the study of the formation of surfactant free microemulsions in the ternary system: water/eugenol/ethanol. The solvent A (water) is miscible with solvent C (ethanol), and the solvent C is miscible with compound B (eugenol), whereas the miscibility of water and eugenol is negligible. The mixture fulfills the basic condition for presenting a "pre-Ouzo" region, thus allowing one to prepare surfactant free microemulsions. In recent years, the development of tailored non-toxic surfactant free microemulsions has undergone a spectacular development due to their potential interest as cargo systems for controlled release of several actives [11–13]. As a consequence, essential oils, such as eugenol, are considered good candidates for the design of cargo systems, which can be used for controlling some disease-vector proliferation, e.g. insects.

Essential oils are easily extractable, eco-friendly, biodegradable compounds, presenting an almost negligible toxicity for mammals. However, they are in general very effective against a wide spectrum of insect pests [14–23]. This is particularly important because it is well recognized that many essential oils derived from plants are toxic, repellent, antifeedant, and/or growth and development inhibitors for arthropods [24–26]. Among these essential oils, eugenol has particular interest due to their strong insecticidal activity against different insect pests [27–29]. Eugenol is the main constituent of several important essential oils such as clove oil, pimenta berry, and bay and cinnamon leaves [30].

Furthermore, several studies have demonstrated that surfactant free microemulsions [31,32] provides the bases for drug solubilisation due to the hydrotropic effect, which involves the solubilisation phenomenon of a poorly soluble solute in a solvent due to the formation of organized dispersed cluster of a second liquid [33]. Thus, it is possible to use this type of systems to improve the solubility of drugs that are poorly soluble in water. This opens important perspectives for the use of surfactant free microemulsions for the encapsulation of pesticides, leading to new biodegradable formulations for pest control that still maintain a relatively high activity.

In this paper, we study of the phase diagram of the ternary mixture water/eugenol/ethanol, and analyze the aggregation phenomena occurring along the one phase region. Furthermore, the encapsulation of a poorly water soluble insecticide (imidacloprid) inside the aggregates formed was studied as proof of concept for future developments of new formulations for pest control.

2. Materials and methods

2.1. Chemicals

Eugenol (IUPAC Name 4-allyl-2-methoxyphenol) (purity ≥99%) was purchased from Sigma-Aldrich (Germany). Chemical structure of eugenol is shown in Scheme 1. Ethanol Absolute (99.5%) was purchased from Panreac (Madrid, Spain). Imidacloprid was

purchased from Sigma-Aldrich (Germany). All the chemical were used without further purification. The ultrapure deionized water (Milli-Q water) used was obtained by a multicartridge purification system (Younglin 370 Series, South Korea) presenting a resistivity higher than 18 MΩ cm and a total organic content lower than 6 ppm.

2.2. Methods

2.2.1. Ternary phase diagram (water/eugenol/ethanol)

The phase diagram was recorded using tubular glass vials (10 ml). The binary mixtures of eugenol and ethanol at different concentrations were prepared by weight and then the weighed amounts of the third component (water) were added. Ternary mixtures with different compositions were studied at 25 °C.

In the two phase region, the preferential partition of ethanol between water and/or eugenol has been quantified using Gas Chromatography Mass Spectrometry Analysis (GC–MS), thus the ethanol content in each component (water and eugenol) was analyzed. For this purpose, a gas chromatograph Agilent 7890A-GC (Agilent Technology-Santa Clara, USA) coupled to an Agilent 5975C inert mass spectrometric detector (MSD) (Agilent Technologies-Santa Clara, USA) was used. Gas chromatography was performed using a SUPELCOWAX® capillary column (length 20 m and inner diameter 0.25 mm). The total content of ethanol in the samples was calculated from the total area of the different peaks corresponding to the presence of ethanol. The calibration was made ad hoc using solutions with an ethanol concentration in the range 1–30 w/w%.

2.2.2. Dynamic Light Scattering (DLS)

Dynamic Light Scattering (DLS) experiments were performed using a Zetasizer Nano ZS Instrument (Malvern Instruments Ltd., Malvern, UK). The DLS measurements were performed at 25 °C using the red line (wavelength, $\lambda = 632$ nm) of a He-Ne laser in a quasi-backscattering configuration (scattering angle, $\theta = 173^{\circ}$). Previously to each measurement, the solutions were filtered in a clean room using a 0.45 μm Nylon membrane (Millex®, USA) to remove the dust particles. The filtered samples were transferred to a quartz measurement cell (Hellma® 6030-OG Model). In DLS experiments we measure the normalized intensity or second-order autocorrelation function, $g^{(2)}(q,t)$, that is related to the field or first-order autocorrelation function, $g^{(1)}(q,t)$, through the Siegert relationship,

$$g^{(2)}(q,t) - 1 = \beta |g^{(1)}(q,t)|^2 \quad (1)$$

where t is the time, $q\left(=(4\pi n/\lambda)\sin\left(\theta/2\right)\right)$ is the wavevector, and n the solution refractive index. In Eq. (1), β is an optical coherence factor and is generally found to be close to 1, except for cases in which the scattered intensity is low. Either because of the low size of the scatterers, low concentration or poor refractive index contrast between the scatterers and the solvent.

3. Results and discussion

3.1. Ternary phase diagram

Ternary mixtures formed by water (W), eugenol (Eu) and ethanol (EtOH) lead to a rich phase diagram in which several regions can be distinguished. Fig. 1 shows the phase diagram, obtained combining the visual observation of the samples, turbidimetry and GC–MS experiments, for the ternary system formed by water (W), eugenol (Eu) and ethanol (EtOH) mixtures in the whole range of weight ratio of the components. It is worth mentioning that ethanol is completely soluble in both water and eugenol, fulfilling the requirements to develop the so-called "pre-Ouzo" effect [34–37]. Different points distributed along the entire phase diagram were studied. In order to study the formation of one phase regions, three different paths were studied. Along the aforementioned paths, the mixtures were prepared keeping constant the weight fractions ratio of two of the components. The three main paths studied are evidenced in the diagram with Roman numeral (from I to III), representing the following mixtures:

- wt% (W)/wt% (EtOH) = 1
- wt% (Eu)/wt% (EtOH) = 1
- wt% (W)/wt% (Eu) = 1

Table 1
Ethanol partitioning between water (EtOH in W) and eugenol (EtOH in Eu) within the two phases region of the phase diagram as was determined by GC–MS.

wt% (W)	wt% (Eu)	wt% (EtOH)	wt% (EtOH in W)	wt% (EtOH in Eu)
25.1 ± 0.2	49.9 ± 0.1	25.0 ± 0.2	50 ± 4	50 ± 4
29.9 ± 0.2	40.1 ± 0.2	30.0 ± 0.2	50 ± 4	50 ± 4
50.1 ± 0.1	25.0 ± 0.2	24.9 ± 0.2	74 ± 6	26 ± 2
39.8 ± 0.2	30.3 ± 0.2	29.9 ± 0.2	56 ± 4	44 ± 3
35.5 ± 0.2	34.8 ± 0.2	29.7 ± 0.2	54 ± 4	46 ± 3
40.0 ± 0.2	39.9 ± 0.2	20.1 ± 0.3	67 ± 4	33 ± 4
44.9 ± 0.1	45.0 ± 0.1	10.1 ± 0.3	70 ± 2	30 ± 1

Furthermore six additional paths in which the weight fraction of ethanol, wt% (EtOH), remained constant (0.1, 0.2, 0.25, 0.4, 0.5 and 0.6), and the weight fractions of water, wt% (W), and eugenol, wt% (Eu), were modified were also studied. These paths are also indicated in the phase diagram: from IV for the Path with lower wt% (EtOH) value (0.1) to IX for the Path with the higher wt% (EtOH) (0.6). Only a detailed discussion of the paths I to III will be presented hereinafter. The study of the paths from IV to IX was carried out to design a more detailed phase diagram.

The analysis of the different samples studied has allowed us to identify two different regions in the phase diagram as a function of the components weight fraction. The first one corresponds to a cloudy multiphase zone in which the ethanol presents either a preferential partitioning in water, or a similar partitioning between both water and eugenol, according to the tie lines obtained on the bases of GC–MS experiments in selected samples. Table 1 shows the results obtained by GC–MS for the partitioning of ethanol between water and eugenol within the two phase region.

Most of the phase diagram, extending from eugenol rich to water rich regions, corresponds to samples formed by a pseudo-single and transparent phase, which is macroscopically homogeneous and thermodynamically stable. This region marks the increase of the co-solubility of water and eugenol due to the addition of ethanol, leading to the formation of a surfactant free microemulsion or real solutions. This was also reported by Marcus et al. [11] for mixtures of water/perfumery molecules/ethanol. It is worth mentioning that the co-solvency in the water/eugenol/ethanol ternary mixtures is rather different to that occurring for the co-solvency phenomenon on polymer solutions. In this case a polymer can be solubilized in a mixture of solvents each of which is not good solvent for the polymer [38]. However, in the ternary mixture studied, the addition of the third component (ethanol), which is mutually soluble with the other two solvents (water and eugenol), leads to the enhancement of the miscibility of the two other solvents.

The co-solvency along three different compositional Paths within the one phase region of the ternary phase diagram was studied using Dynamic Light Scattering (DLS). The three Paths studied merge at a point in the onset on the two phase region where ethanol does not show any preferential distribution neither for the water nor for the eugenol (ethanol weight content in water 50 ± 4% w/w as was determined by GC–MS). The composition in which the three compositional paths merge contains the same weight fraction of the three components (33.3% w/w). The increase of the eugenol

Table 2
Different regions appearing along Path I as function of the weight fraction of eugenol, wt% (Eu).

Region	wt% (Eu)	Phase
I.a	25<	Monophasic
I.b	25–35	"Pre-Ouzo"
I.c	35–50	Biphasic (No preferential distribution EtOH)
I.d	>50	Biphasic (EtOH preferentially distributed in Eu)

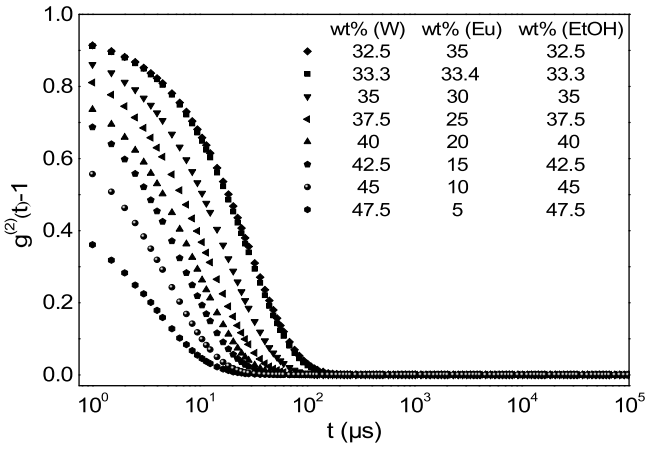

Fig. 2. DLS intensity auto-correlation functions for monophasic mixtures and "pre-Ouzo" along the path I. Legend shows the weight fractions (wt%) of the components.

content beyond this threshold concentration destabilizes the mixtures, leading to phase separation.

3.2. Compositional paths

3.2.1. Path I. wt% (W)/wt% (EtOH) = 1

In this first path we keep constant the ratio between water and ethanol. Table 2 summarize the different regions found along this path as a function of the weight fraction of eugenol. Four different regions of the phase diagram were identified.

Fig. 2 shows the intensity autocorrelation functions obtained by DLS experiments as the eugenol weight fraction is increased. It is worth mentioning that, as expected, the pure liquids do not show any correlation in DLS experiments.

The intensity autocorrelation functions of the single phase samples show an exponential behavior characterized by an average decay time, τ. There are two possible explanations for this behaviour: one is related to the appearance of co-solvency phenomena leading to the formation of surfactant free microemulsions [7–9], whereas the other one involves the existence of large concentration fluctuations due to the proximity to a liquid–liquid critical point [39,40]. In order to rule out one of the aforementioned scenarios, several pseudo-single phase mixtures were studied in the temperature range 20–50 °C, and no evidence of destabilization of the samples was found. Therefore it is possible to rule out the critical concentration fluctuations as the source of the intensity correlation in the pseudo-single phase region of the ternary phase diagram under study. Thus, we must conclude that the intensity correlation found in the DLS experiments is due to the diffusion of nano-structures (clusters, micelles or droplets) dispersed in the continuous liquid phase. A further confirmation of this scenario was obtained by Dynamic Light Scattering (DLS) measurements in the aforementioned temperature range. Fig. 3 shows the autocorrelation functions obtained at different temperatures for one of the samples with a 33.3 wt% w/w of each component ("pre-Ouzo" region). The results pointed out that the change of the temperature does not affect the character of the autocorrelation function, that

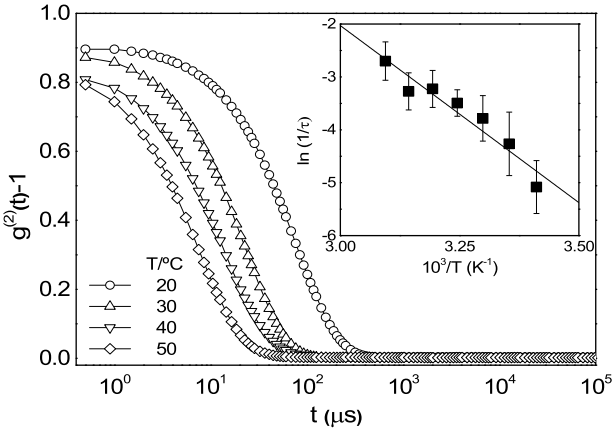

Fig. 3. DLS intensity autocorrelation function at different temperature for a mixture with a 33.3 wt% of each component. The inserted figure represents the Arrhenius plot for the dependence of the characteristic times on the temperature, being the solid symbols are the experimental data and the solid line is the fitting to an Arrhenius' law.

for all the temperatures present an exponential decay which can be characterized by an average decay time, τ. In the case of Brownian diffusion the first-order autocorrelation function follows an exponential decay with time.

$$g^{(1)}(q,t) = \exp(-t/\tau) = \exp(-Dq^2 t) \quad (2)$$

where the inverse decay time, 1/τ, is directly related to the self-diffusion coefficient, D. Considering that usually the samples present some degree of polydispersity [41] both τ and D must be considered as average quantities. The self-diffusion coefficient for spherical Brownian objects diffusing in a Newtonian medium can be related with the hydrodynamic radius, R_H, through the Stokes-Einstein equation [42]

$$D = \frac{k_B T}{6\pi\eta R_H} \quad (3)$$

where k_B is the Boltzmann constant, T is the absolute temperature and η the shear viscosity of the solvent, in our case the continuous phase.

Eq. (3) is strictly correct at infinite dilution, as a consequence is customary to use an apparent diffusion coefficient, D_{app}, and hydrodynamic radius, $R_{H,app}$, for a finite concentration.

According to Eqs. (2) and (3), it is expected that the inverse decay time should follow with the temperature an Arrhenius type behavior, essentially corresponding to the one of the continuous phase shear viscosity variation with the temperature.

$$\frac{1}{\tau} \approx A_0 e^{-E_a/(k_B T)} \quad (4)$$

where A_0 is a pre-exponential factor and E_a is the activation energy for the diffusive transport. The insert in Fig. 3 show the Arrhenius plot with values $A_0 = 69 \pm 11\ s^{-1}$ and $E_a = 56 \pm 11$ kJ/mol.

In summary, the dynamics observed by DLS experiments and their temperature variation can be explained as due to the concentration fluctuations because the formation of aggregates or cluster that present a Brownian diffusion in a continuous phase [7–9].

With regards to the eugenol content the results shown in Fig. 4 point out two different effects: (a) the average decay time increases with the eugenol weight fraction, and (b) the scattered intensity becomes higher as the weight content of eugenol is increased

Due to the fact that the real shape, size or the kinetic of formation of the nanosized droplets (clusters) formed may change very abruptly within the phase diagram and that the viscosity, refractive index and even the mere nature of the continuous phase may also change from point to point in the phase diagram, we decided

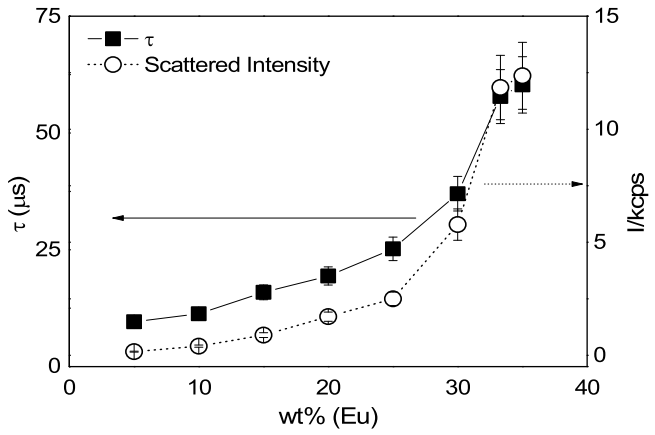

Fig. 4. DLS characteristic time (left axis) and scattered intensity (right axis) dependences on the weight fraction of eugenol (wt% (Eu)) for ternary monophasic and "pre-Ouzo" mixtures along the path I. The solid lines are guides for the eyes.

Table 3
Different regions appearing along the Path II as function of the weight fraction of water, wt% (W).

Region	wt% (W)	Phase
II.a	30<	Monophasic
II.b	30–35	"Pre-Ouzo"
II.c	35–50	Biphasic (No preferential distribution EtOH)
II.d	>50	Biphasic (EtOH preferentially distributed in W)

not to make the discussion in terms of the hydrodynamic radius, $R_{H,app}$, or the diffusion coefficient, $D_{app} = 1/\tau q^2$, but in terms of the bare inverse average decay time, $1/\tau$. So hereinafter we will focus the discussion over the behavior of the characteristic times and scattered intensities of the concentration fluctuations. It should be understood that longer τ values must correspond to systems that are close to the phase separation, in turn this imply an increase in the scattered intensity and sample turbidity. The approach to the onset of the two-phase region [43] must lead to an increase of the size of the droplets, or in other words concentration fluctuations that span a larger spatial scale, which means longer τ values and higher scattered intensities.

A sudden increase of the scattered intensity as the system approach the phase separation can be explained considering the appearance of a "pre-Ouzo" region in which the pseudo-single phase consist in two different pseudo-phases, the former one enriched in eugenol, and the other rich in water [7,9]. Thus, the scattered intensity values (Fig. 4) indicate that the aforementioned "pre-Ouzo" region appears for eugenol concentrations above 30 wt%. The increase of the scattered intensity for mixtures far from the critical point was discussed by Rubio et al. [44,45] in terms of local concentrations different of the global ones (concentration fluctuations). This concept is not different from the formation of the nanoscopic pseudo-phases of the "pre-Ouzo" region, although it can be also understood as the onset of formation of a surfactant free microemulsion [46].

3.2.2. Path II. wt% (Eu)/wt% (EtOH) = 1

We have studied a second set of samples containing a constant ratio between the content of eugenol and of ethanol equal to unity, and increasing the water content. Table 3 summarizes the different regions along the path II.

Fig. 5a shows the intensity autocorrelation functions obtained for monophasic and "pre-Ouzo" samples with an increasingly water content.

The shape of the intensity autocorrelation functions is similar to that found in path I (Fig. 2). The increase of the water content

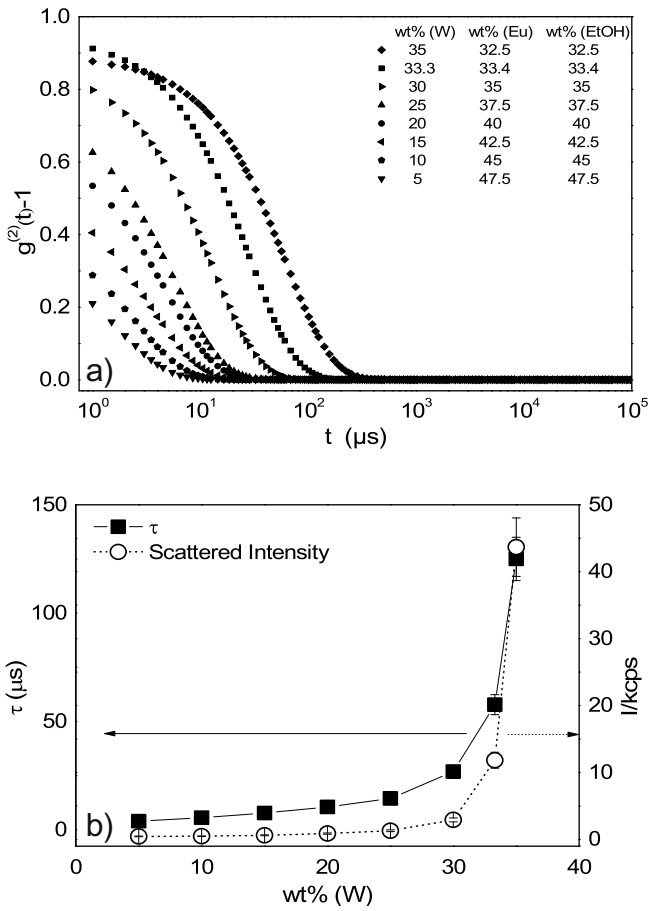

Fig. 5. (a) DLS intensity auto-correlation functions for monophasic and "pre-Ouzo" mixtures along the path II. Legend shows the weight fractions (wt%) of the components. (b) DLS characteristic time (left axis) and scattered intensity (right axis) dependences on the weight fraction of water (wt% (W)) for ternary monophasic and "pre-Ouzo" mixtures along the path II. The solid lines are guides for the eyes.

Table 4
Different regions appearing along the path III as function of the weight fraction of ethanol, wt% (EtOH).

Region	wt% (EtOH)	Phase
III.a	20<	Biphasic (EtOH preferentially distributed in W)
III.b	20–30	Biphasic (No preferential distribution EtOH)
III.c	30–40	"Pre-Ouzo"
III.d	>40	Monophasic

shifts the functions to longer times (see Fig. 5b) as it happened in Path I with the increase of eugenol, and the explanation may follow the same arguments, except that now the continuous phase must be the eugenol, at least for the low water content mixtures. In the two paths studied, the system approached the two phase region as the ethanol content decreases. Therefore, we can conclude that there is a critical ethanol concentration below which there is no water-eugenol co-solvency.

3.2.3. Path III. wt% (W)/wt% (Eu) = 1

The above conclusion can be more clearly seen by measuring a set of samples where the weight ratio water/eugenol remain equal to unity, and increasing the concentration of ethanol (Fig. 6a). Table 4 summarizes the different regions along this path.

In this third path, the characteristic time decreases as the ethanol content increases due to the enhanced miscibility of the mixture (Fig. 6b). Furthermore, the strong decrease of the coherence observed in the intensity autocorrelation functions as the

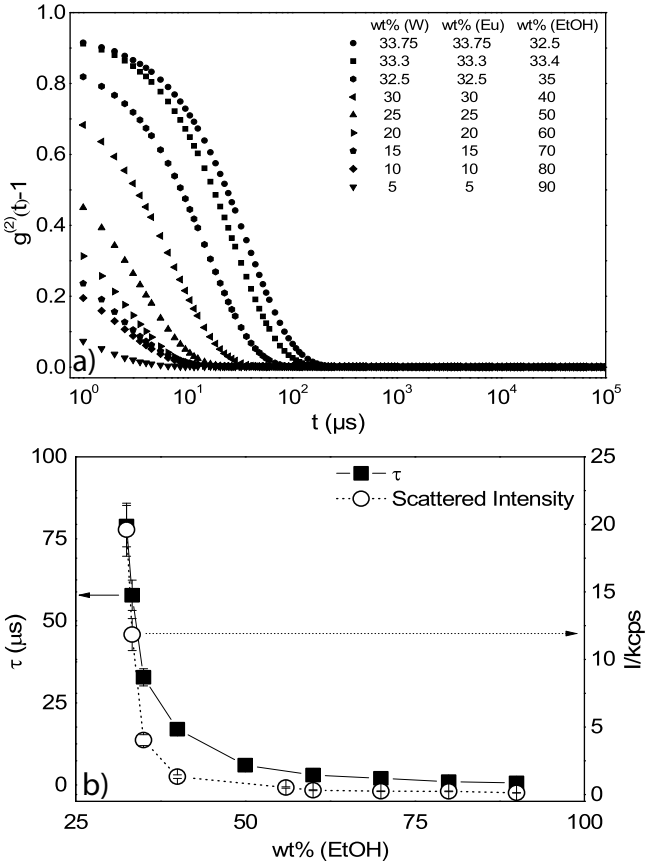

Fig. 6. (a) DLS intensity auto-correlation functions for monophasic and "pre-Ouzo" mixtures along the path III. Legend shows the weight fractions (wt%) of the components. (b) DLS characteristic time (left axis) and scattered intensity (right axis) dependences on the weight fraction of ethanol (wt% (EtOH)) for ternary monophasic and "pre-Ouzo" mixtures along the path III. The solid lines are guides for the eyes.

ethanol concentration increases suggests a transition between a surfactant free microemulsion to a real solution. In order to deepen in the phenomenon, we have analyzed the τ dependence on the weight ratio of water and ethanol, and the scattered intensity for mixtures in which the weight ratio eugenol/ethanol is equal to unity (Fig. 5b) and the weight ratio water/eugenol is equal to 1 (Fig. 6b), respectively. In this first case (Fig. 5b) the behavior is similar that of mixtures in which the weight ratio water/ethanol was close to 1. As the water content is increased the sample becomes close to the destabilization region, the "pre-Ouzo" region being located at a water content above 30 wt%. Beyond this threshold the size of the concentration fluctuations, and thus the scattered intensity, increase as the system approach the destabilization. The destabilization of the microemulsions appears for water content between 35 and 40 wt%, and in this region there is no preference for the partitioning of the ethanol in water or in eugenol. This has been confirmed by the GC–MS results that show that the ethanol content in the water-rich phase is 56 ± 4 wt% of the total ethanol content in the mixture containing 40 wt% of water. A further increase of the water content leads to a preferential partitioning of the ethanol on the water rich phase up to 75 wt%.

The above discussion allowed us to suggest the importance of the ethanol content in the co-solvency phenomena here presented. Fig. 6b presents the characteristic time and the scattered intensity for samples with a water/eugenol weight ratio constant and equal to unity and with increasingly ethanol concentrations. These results confirm the key role of the ethanol, suggested by the results of Paths I and II for ensuring the water/eugenol co-solvency. Notice that the

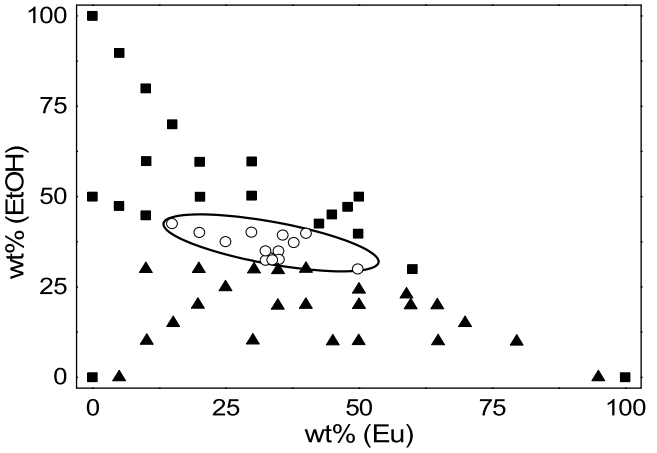

Fig. 7. 2D-expansion of the phase diagram for water–eugenol–ethanol ternary mixtures. Three different regions can be observed from the samples analyzed: (■) stable regions (▲) instable regions (○) "pre-Ouzo" regions. Notice that the ellipse marks the boundaries of the "pre-Ouzo" region.

behavior in Fig. 6b looks like opposite to Figs. 4 and 5 b, indicating that decreasing the ethanol concentration brings the system close to the phase separation.

3.2.4. "Pre-Ouzo" region

At ethanol content close to 40 wt% the systems enters into the "pre-Ouzo" region as indicated by the strong increase in the scattered intensity. Below that ethanol content the mixture forms a surfactant free microemulsion with no preferential partition of the ethanol between water and eugenol: 54 ± 4 wt% is the ethanol content in the water rich phase for samples containing an overall 30 wt% of ethanol. Further decrease of total ethanol content in the mixtures leads to a preferential partitioning in the water rich phase, reaching the ethanol content water values closer to 70 wt% w/w of its total content as the water content is increased till 45 wt%. Furthermore, the results pointed out that for high ethanol contents the mixtures are thermodynamically stable, in agreement with the molecular dynamics simulations for the water/octanol/ethanol ternary mixture [8].

For a total content in the range of 30–40 wt% a "pre-Ouzo" region exists in which the co-solvency water-eugenol is enhanced. Only when the weight fraction of ethanol is higher than 40 wt% appears pseudo-single phase mixtures. Fig. 7 shows a 2D-expansion of the phase diagram for water – eugenol- ethanol ternary mixtures on the basis of the samples analyzed in which the stability, including "pre-ouzo" one, and the instability regions are shown according to the scattered intensity for the samples.

3.3. Sizes of the aggregates

We have discussed that by DLS, it is possible to estimate the dimensions of the aggregates or cluster formed in the solution (Eqs. (2) and (3)). However, for a complex system such the one here studied an uncertainty associated with the nature of the continuous phase makes difficult to estimate the real size of the aggregates. In order to obtain an estimation of the size, we have chosen the wavevector and viscosity corresponding to the continuous phase for the samples along Paths I–III. Thus, for samples along Path I and III, the continuous phase is assumed to be water, whereas for samples along Path II the continuous phase is considered to be eugenol. Fig. 8 shows a 3D plot including the 2D-expansion of the phase diagram in the monophasic and "pre-Ouzo" regions for water–eugenol–ethanol ternary mixtures and the corresponding

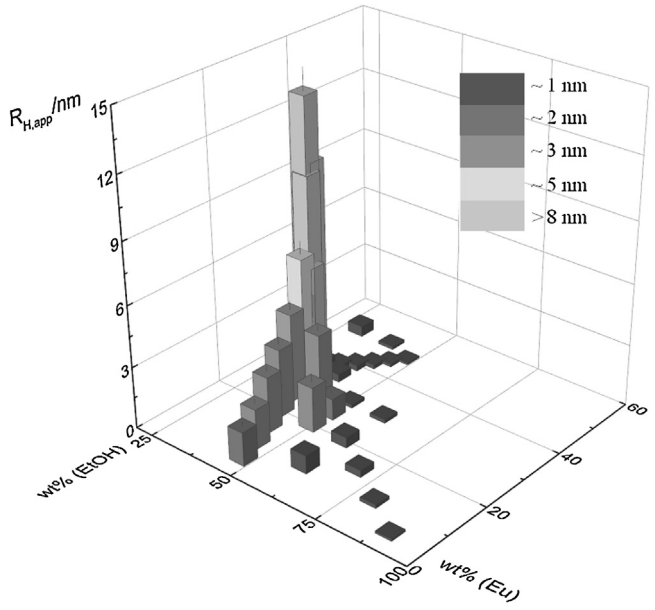

Fig. 8. Apparent hydrodynamic radius estimated from equation 3 for the different samples studies according 2D-expansion of the phase diagram for water–eugenol–ethanol. The gray level represents different hydrodynamic radius range (see legend).

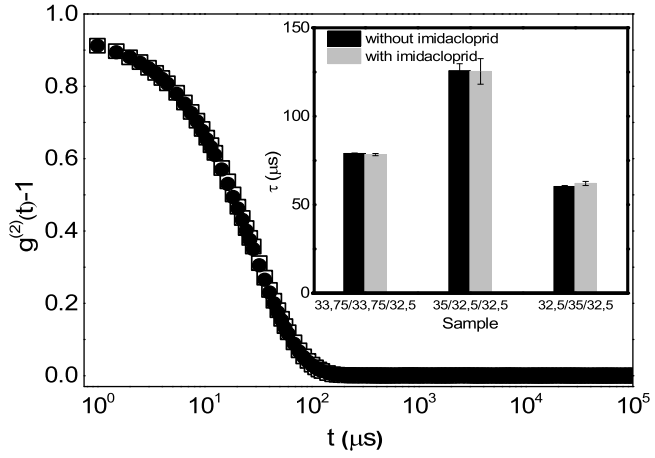

Fig. 9. (a) DLS intensity auto-correlation functions for a ternary mixture containing a composition of 32.5/35/32.5 wt% of water, eugenol and ethanol, respectively in absence (□) and presence (●) of imidacloprid (0.3 wt%). The inserted figure represents the DLS characteristic average decay time for different ternary mixtures water/eugenol/ethanol. The x axis indicates the weight fraction of the different components as wt% (W)/wt% (Eu)/wt% (EtOH).

apparent hydrodynamic radius estimated for the aggregates using Eq. (2).

The results point out that the radius of the aggregates increase as the "pre-Ouzo" region is approached for samples with 30–40 wt% of ethanol. The increase of the ethanol weight fraction or the decrease of the weight fraction of either water or eugenol leads to the decrease of the size of the aggregates.

3.4. Solubility of a model insecticide in "pre-Ouzo" mixtures

Some tests of the solubilization capacity within the "pre-Ouzo" region of a model insecticide have been performed. The inclusion of imidacloprid in a final concentration of 0.3 wt% does not affect to the stability of the samples. Fig. 9 shows that the inclusion of the insecticide does not modify the intensity autocorrelation function. Therefore, we can conclude that the microemulsion favors the solubility of a poorly soluble drug without affecting on its stability (hydrotropic effect). This is more clearly demonstrated in the inserted panel in Fig. 9. The absence of any appreciable change in the characteristic average decay time associated with the aggregation phenomena occurring in the "pre-Ouzo" region confirms the absence of any significant effect of the imidacloprid on the stability of the formulations, and opens new perspectives for the fabrication of delivery platforms for the pest control.

The present formulation has shown a very good activity against mosquito in laboratory tests [45].

4. Conclusions

In this work we present a study of the enhancement of co-solvency of water and an essential oil, eugenol, due to the addition of ethanol. The enlightenment of the phase diagram of the ternary mixture have evidenced the formation of one pseudo-single phase region and a multiphase region in which different partitioning of ethanol in eugenol and water was found. The transition from the multiphase regions to the pseudo-single phase one is marked by the appearance of a "pre-Ouzo" border region in which the ethanol content is in the 30–40 wt% range. The results have also suggested a possible transition in the pseudo-single phase region from a surfactant free microemulsion to a real solution as the ethanol content is increased. The highest ethanol content favors the formation of thermodynamically stable systems. Thus, the results have pointed out the critical role of the ethanol content for favoring the co-solvency of eugenol and water,

The surfactant free microemulsions obtained allows the solubilization of a model insecticide (hydrotropic effect) such as the imidacloprid, thus the studies of this intriguing ternary system water/eugenol/ethanol could be extended in future for the fabrication of delivery systems. These studies can offer some promising approach to optimize the encapsulation of natural compounds for the pest control.

Acknowledgements

This work was funded in part by MINECO under grants FIS-2012-38231-C02-01 and FIS 2014-62005-EXP, by EU under Marie Curie ITN CoWet, and performed in the framework of the COST Actions CM-1101 and MP-1106. A.L. has received financial support from CONICET through an International Postdoctoral Fellowship and the National Agency for Science and Technology Promotion of Argentina (ANPCYT) through a Scientific and Technological Project (PICT 2012-2453). AL is especially grateful to Dr. Hector Masuh and Dr. Eduardo Zerba particularly for their support in the presentation at the postdoctoral fellowship. E.G. is grateful to the MINECO for the JdC contract. We are grateful to C.A.I. de Espectrocospia y Correlación and to C.A.I. de Espectrometría de Masas, of the U.C.M. for the use of their facilities.

References

[1] I. Danielsson, B. Lindman, The definition of a microemulsion, Colloids Surf. 3 (1981) 391–392.
[2] P.A. Winsor, Hydrotropy, solubilisation and related emulsification processes, Trans. Faraday Soc. 44 (1948) 376–398.
[3] G.D. Smith, C.E. Donelan, R.E. Barden, Oil-continuous microemulsions composed of hexane, water, and 2-propanol, J. Colloid Interface Sci. 60 (1977) 488–496.
[4] V. Fischer, J. Marcus, D. Touraud, O. Diat, W. Kunz, Toward surfactant free and water-free microemulsions, J. Colloid Interface Sci. 453 (2015) 186–193.
[5] J. Xu, A. Yin, J. Zhao, D. Li, W. Hou, Surfactant free microemulsion composed of oleic acid, *n*-propanol, and H_2O, J. Phys. Chem. B 117 (2013) 450–456.
[6] M.L. Klossek, D. Touraud, W. Kunz, Eco-solvents—cluster-formation, surfactantless microemulsions and facilitated hydrotropy, Phys. Chem. Chem. Phys. 15 (2013) 10971–10977.

[7] O. Diat, M.L. Klossek, D. Touraud, B. Deme, I. Grillo, W. Kunz, T. Zemb, Octanol-rich and water-rich domains in dynamic equilibrium in the pre-Ouzo region of ternary systems containing a hydrotrope, J. Appl. Crystallogr. 46 (2013) 1665–1669.
[8] S. Schöttl, J. Marcus, O. Diat, D. Touraud, W. Kunz, T. Zemb, D. Horinek, Emergence of surfactant free micelles from ternary solutions, Chem. Sci. 5 (2014) 2949–2954.
[9] M.L. Klossek, D. Touraud, T. Zemb, W. Kunz, Structure and solubility in surfactant free microemulsions, ChemPhysChem 13 (2012) 4116–4119.
[10] A.R. Tehrani-Bagha, A. Viladot, K. Holmberg, L. Nordstiern, An Ouzo emulsion of toluene in water characterized by NMR diffusometry and static multiple light scattering, Colloids Surf. A 494 (2016) 81–86.
[11] J. Marcus, M.L. Klossek, D. Touraud, W. Kunz, Nano-droplet formation in fragrance tinctures, Flavour Fragr. J. 28 (2013) 294–299.
[12] J. Marcus, M. Müller, J. Nistler, D. Touraud, W. Kunz, Nano-droplet formation in water/ethanol or isopropanol/mosquito repellent formulations, Colloids Surf. A 458 (2014) 3–9.
[13] J. Drapeau, M. Verdier, D. Touraud, U. Krçckel, M. Geier, A. Rose, W. Kunz, Effective insect repellent formulation in both surfactantless and classical microemulsions with a long-Lasting protection for human beings, Chem. Biodivers. 6 (2009) 934–947.
[14] R. Tisserand, T. Balacs, Essential Oils Safety: A Guide for Health Care Professionals, Churchill Livingstone, London-United Kingdom, 1995.
[15] M.B. Isman, Plant essential oils for pest and disease management, Crop. Prot. 19 (2000) 603–608.
[16] M. Isman, Pesticides based on plant essential oils, Pestic. Outlook 10 (1999) 68–72.
[17] E. Shaaya, A. Rafaeli, Essential oils as biorational insecticides potency and mode of action, in: I. Ishaaya, R. Nauen, R. Horowitz (Eds.), Insecticides Design Using Advanced Technologie, Springer, Berlin-Germany, 2007, pp. 249–261.
[18] A. Amer, H. Mehlhorn, Larvicidal effects of various essential oils against *Aedes*, *Anopheles*, and *Culex* larvae (Diptera, Culicidae), Parasitol. Res. 99 (2006) 466–472.
[19] A. Amer, H. Mehlhorn, Repellency effect of forty-one essential oils against *Aedes*, *Anopheles*, and *Culex* mosquitoes, Parasitol. Res. 99 (2006) 478–490.
[20] A. Bagvan, A.A. Rahuman, C. Kamraj, K. Geetha, Larvicidal activity of saponin from *Achyranthes aspera* against *Aedes aegypti* and *Culex quinquefasciatus* (Diptera: Culicidae), Parasitol. Res. 103 (2008) 223–229.
[21] A. Lucia, E. Zerba, H. Masuh, Knockdown and larvicidal activity of six monoterpenes against *Aedes aegypti* (Diptera: Culicidae) and their structure-activity relationships, Parasitol. Res. 112 (2013) 4267–4272.
[22] A. Lucia, L. Juan, E. Zerba, L. Harrand, M. Marcó, H. Masuh, Validation of models to estimate the fumigant and larvicidal activity of *Eucalyptus* essential oils against *Aedes aegypti* (Diptera: Culicidae), Parasitol. Res. 110 (2012) 1675–1686.
[23] A. Lucia, S. Licastro, E. Zerba, P.A. González-Audino, H. Masuh, Sensitivity of *Aedes aegypti* adults (Diptera: Culicidae) to the vapors of *Eucalyptus* essential oils, Bioresour. Technol. 100 (2009) 6083–6087.
[24] R.A. Weinzieri, D. Palevitch, L. Craker, Volatile oils as potential insecticides, Herb. Spice Med. Plant Dig. 12 (1994) 1–8.
[25] J.R. Coats, Risks from natural versus synthetic insecticides, Annu. Rev. Entomol. 39 (1994) 489–515.
[26] R.A. Weinzieri, Botanical insecticides, soaps, and oils, in: J.E. Rechcigl, N.A. Rechcigl (Eds.), Biological and Biotechnological Control of Insect Pests, Lewis, Boca Raton-United States of America, 2000.
[27] A.N. Moretti, E.N. Zerba, R.A. Alzogaray, Behavioral and toxicological responses of *Rhodnius prolixus* and *Triatoma infestans* (Hemiptera: Reduviidae) to 10 monoterpene alcohols, J. Med. Entomol. 50 (2013) 1046–1054.
[28] R.A. Alzogaray, V. Sfara, A.N. Moretti, E.N. Zerba, Behavioural and toxicological responses of *Blattella germanica* (Dictyoptera: Blattellidae) to monoterpenes, Eur. J. Entomol. 110 (2013) 247–252.
[29] A.C. Toloza, C. Vasenna, M.I. Picollo, Ovicidal and adulticidal effects of monoterpenoids against permethrin-resistant human lice, Pediculus humanus capitis, Med. Vet. Entomol. 22 (2008) 335–339.
[30] E. Guenther, The Essential Oils, Van Nostrand, Inc., Princeton-United States of America, 1949.
[31] J.J. Booth, S. Abbott, S. Shimizu, Mechanism of hydrophobic drug solubilization by small molecule hydrotropes, J. Phys. Chem. B 116 (2012) 14915–14921.
[32] P. Simamora, J.M. Alvarez, S.H. Yalkowsky, Solubilization of rapamycin, Int. J. Pharm. 1 (2001) 25–29.
[33] A.B. Morais, C. Jayakumar, N.N. Gandhi, Hydrotropic effect and thermodynamic analysis on the solubility and mass transfer coefficient enhancement of ethylbenzene, Korean J. Chem. Eng. 30 (2013) 925–930.
[34] S.A. Vitale, J.L. Katz, Liquid droplet dispersions formed by homogeneous liquid–liquid nucleation: the Ouzo effect, Langmuir 19 (2003) 4105–4110.
[35] N.L. Sitnikova, R. Sprik, G. Wegdam, E. Eiser, Spontaneously formed *trans*-anethol/water/alcohol emulsions: mechanism of formation and stability, Langmuir 21 (2005) 7083–7089.
[36] D. Carteau, I. Pianet, P. Brunerie, B. Guillemat, D.M. Bassani, Probing the initial events in the spontaneous emulsification of *trans*-anethole using dynamic NMR spectroscopy, Langmuir 23 (2007) 3561–3565.
[37] R. Botet, The Ouzo effect, recent developments and application to therapeutic drug carrying, J. Phys.: Conf. Series 352 (2012) 012047.
[38] I. Katime, J.R. Ochoa, L.C. Cesteros, J. Peñafiel, Polymer cosolvent systems. 3. PMMA(3)/CCl4 (1)/*n*-butyl chloride(2), Polym. Bull. 6 (1982) 429–436.
[39] M.P. Hernández, F. Ortega, R.G. Rubio, Crossover critical phenomena in an aqueous electrolyte solution: light scattering, density and viscosity of the 3-methylpyridine-water-NaBr system, J. Chem. Phys. 119 (2003) 4428–4436.
[40] R.G. Rubio, F. Ortega, Critical behaviour of complex systems, J. Phys.: Condens. Matter 12 (2000) A459–A463.
[41] If the polydispersity is too high the diffusion coefficient becomes dependent of the wavevector, D(q).
[42] R. Pecora, Dynamic Light Scattering: Applications of Photon Correlation Spectroscopy, Plenum Press, United States of America, 1985.
[43] E. Guzmán, S. Llamas, A. Maestro, L. Fernández-Peña, A. Akanno, R. Miller, F. Ortega, R.G. Rubio, Polymer–surfactant systems in bulk and at fluid interfaces, Adv. Colloid Interface Sci. (2016), http://dx.doi.org/10.1016/j.cis.2015.11.001.
[44] R.G. Rubio, M.G. Prolongo, M. Díaz-Peña, J.A.R. Renuncio, Local composition in real mixtures of simple molecules, J. Phys. Chem. 91 (1987) 1177–1184.
[45] R.G. Rubio, M. Caceres, R.M. Masegosa, L. Andeolliball, M. Costas, D. Patterson, Mixtures with W-shape CPE curves—a light scattering study, Ber. Bunsen Phys. Chem. 93 (1989) 48–56.
[46] T.F. Tadros, Emulsion Science and Technology, Wiley-VCH Verlag, Berlin, 2009.